



## Experimental demonstration of Generalized Phase Contrast based Gaussian beam-shaper

Tauro, Sandeep; Bañas, Andrew Rafael; Palima, Darwin; Glückstad, Jesper

*Published in:*  
Optics Express

*Link to article, DOI:*  
[10.1364/OE.19.007106](https://doi.org/10.1364/OE.19.007106)

*Publication date:*  
2011

*Document Version*  
Publisher's PDF, also known as Version of record

[Link back to DTU Orbit](#)

*Citation (APA):*  
Tauro, S., Bañas, A. R., Palima, D., & Glückstad, J. (2011). Experimental demonstration of Generalized Phase Contrast based Gaussian beam-shaper. *Optics Express*, 19(8), 7106-7111.  
<https://doi.org/10.1364/OE.19.007106>

---

### General rights

Copyright and moral rights for the publications made accessible in the public portal are retained by the authors and/or other copyright owners and it is a condition of accessing publications that users recognise and abide by the legal requirements associated with these rights.

- Users may download and print one copy of any publication from the public portal for the purpose of private study or research.
- You may not further distribute the material or use it for any profit-making activity or commercial gain
- You may freely distribute the URL identifying the publication in the public portal

If you believe that this document breaches copyright please contact us providing details, and we will remove access to the work immediately and investigate your claim.

# Experimental demonstration of Generalized Phase Contrast based Gaussian beam-shaper

Sandeep Tauro, Andrew Bañas, Darwin Palima and Jesper Glückstad\*

DTU Fotonik, Department of Photonics Engineering, Technical University of Denmark  
Ørstedss Plads 343, DK-2800 Kgs. Lyngby, Denmark

\*jesper.gluckstad@fotonik.dtu.dk

[www.ppo.dk](http://www.ppo.dk)

**Abstract:** We report the first experimental demonstration of Gaussian beam-shaping based on the Generalized Phase Contrast (GPC) approach. We show that, when using a dynamic spatial light modulator (SLM), this approach can rapidly generate arbitrarily shaped beams. Moreover, we demonstrate that low-cost binary-phase optics fabricated using photolithography and chemical etching techniques can replace the SLM in static and high power beam shaping applications. The design parameters for the binary-phase elements of the module are chosen according to the results of our previously conducted analysis and numerical demonstrations [Opt. Express **15**, 11971 (2007)]. Beams with a variety of cross-sections such as circular, rectangular and square, with near flat-top intensity distributions are demonstrated. GPC-based beam shaping is inherently speckle-free and the shaped beams maintain a flat output phase. The non-absorbing components used in this beam-shaping approach have a high-damage-threshold and are thus ideally suited for high power applications.

© 2011 Optical Society of America

**OCIS codes:** (070.6110) Spatial filtering; (140.3300) Laser beam shaping; (100.1390) binary phase-only filters; (070.6120) Spatial light modulators.

---

## References and links

1. F. M. Dickey, and S. C. Holswade, *Laser Beam Shaping: Theory and Techniques* (Marcel Dekker, New York, 2000).
2. H. Herzig, *Micro-Optics: Elements, Systems & Applications* (Taylor and Francis Ltd, London (1997).
3. W. B. Veldkamp, "Laser beam profile shaping with binary diffraction grating," Opt. Commun. **38**(5-6), 381–386 (1981).
4. A. J. Caley, M. J. Thomson, J. Liu, A. J. Waddie, and M. R. Taghizadeh, "Diffractive optical elements for high gain lasers with arbitrary output beam profiles," Opt. Express **15**(17), 10699–10704 (2007).
5. J. Cordingley, "Application of a binary diffractive optic for beam shaping in semiconductor processing by lasers," Appl. Opt. **32**(14), 2538–2542 (1993).
6. C. Dorner, "High-damage-threshold beam shaping using binary phase plates," Opt. Lett. **34**(15), 2330–2332 (2009).
7. M. A. Karim, A. M. Hanafi, F. Hussain, S. Mustafa, Z. Samberid, and N. M. Zain, "Realization of a uniform circular source using a two-dimensional binary filter," Opt. Lett. **10**(10), 470–471 (1985).
8. R. Brandstetter, and K. Leib, "Fabrication of a binary phase only filter (BPOF) on transparency film," Opt. Laser Technol. **23**(4), 247–250 (1991).
9. J. Yang, and M. Wang, "Analysis and optimization on single-zone binary flat-top beam shaper," Opt. Eng. **42**(11), 3106–3113 (2003).
10. J. S. Liu, and M. R. Taghizadeh, "Iterative algorithm for the design of diffractive phase elements for laser beam shaping," Opt. Lett. **27**(16), 1463–1465 (2002).
11. Y. Lin, T. J. Kessler, and G. N. Lawrence, "Distributed phase plates for super-Gaussian focal-plane irradiance profiles," Opt. Lett. **20**(7), 764–766 (1995).
12. X. Deng, Y. Li, D. Fan, and Y. Qiu, "Pure-phase plates for super-Gaussian focal-plane irradiance profile generations of extremely high order," Opt. Lett. **21**(24), 1963–1965 (1995).
13. X. Tan, B. Y. Gu, G. Z. Yang, and B. Z. Dong, "Diffractive phase elements for beam shaping: a new design method," Appl. Opt. **34**(8), 1314–1320 (1995).
14. J. Glückstad, and D. Palima, "Generalized Phase Contrast: Applications in Optics and Photonics," Springer Series in Optical Sciences **146**, (2009) 310.
15. F. Zernike, "How I discovered phase contrast," Science **121**(3141), 345–349 (1955).

16. P. J. Rodrigo, V. R. Daria, and J. Glückstad, "Real-time interactive optical micromanipulation of a mixture of high- and low-index particles," *Opt. Express* **12**(7), 1417–1425 (2004).
17. V. R. Daria, P. J. Rodrigo, and J. Glückstad, "Dynamic array of dark optical traps," *Appl. Phys. Lett.* **84**(3), 323–325 (2004).
18. P. J. Rodrigo, L. Gammelgaard, P. Bøggild, I. Perch-Nielsen, and J. Glückstad, "Actuation of microfabricated tools using multiple GPC-based counterpropagating-beam traps," *Opt. Express* **13**(18), 6899–6904 (2005).
19. E. Papagiakoumou, F. Anselmi, A. Begue, V. de Sars, J. Glückstad, E. Y. Isacoff, and V. Emiliani, "Scanless two-photon excitation of channelrhodopsin-2," *Nat. Methods* **7**(10), 848–854 (2010).
20. P. C. Mogensen, R. L. Eriksen, and J. Glückstad, "High capacity optical encryption system using ferro-electric spatial light modulators," *J. Opt. A, Pure Appl. Opt.* **3**(1), 10–15 (2001).
21. P. C. Mogensen, and J. Glückstad, "Phase-only optical decryption of a fixed mask," *Appl. Opt.* **40**(8), 1226–1235 (2001).
22. P. J. Rodrigo, D. Palima, and J. Glückstad, "Accurate quantitative phase imaging using generalized phase contrast," *Opt. Express* **16**(4), 2740–2751 (2008).
23. D. Palima, C. A. Alonzo, P. J. Rodrigo, and J. Glückstad, "Generalized phase contrast matched to Gaussian illumination," *Opt. Express* **15**(19), 11971–11977 (2007).
24. D. Palima, and J. Glückstad, "Gaussian to uniform intensity shaper based on generalized phase contrast," *Opt. Express* **16**(3), 1507–1516 (2008).
25. C. Maurer, A. Jesacher, S. Bernet, and M. Ritsch-Marte, "What Spatial Light modulators can do for optical microscopy," *Laser Photon. Rev.* **5**(1), 81–101 (2011).
26. J. Glückstad, and P. C. Mogensen, "Reconfigurable ternary-phase array illuminator based on the generalised phase contrast method," *Opt. Commun.* **173**(1-6), 169–175 (2000).
27. D. Palima, and J. Glückstad, "Multi-wavelength spatial light shaping using generalized phase contrast," *Opt. Express* **16**(2), 1331–1342 (2008).
28. Z. Kuang, W. Perrie, J. Leach, M. Sharp, S. P. Edwardson, M. Padgett, G. Dearden, and K. G. Watkins, "High throughput diffractive multi-beam femtosecond laser processing using a spatial light modulator," *Appl. Surf. Sci.* **255**(5), 2284–2289 (2008).

## 1. Introduction

Laser beams suitably shaped into different geometric patterns and intensity distributions are valuable for a plurality of research and industrial applications. Many applications employing specifically tailored beams outperform those that directly apply the Gaussian beam profiles emitted by most lasers. As a consequence, there is an active utilization of beam shaping techniques in areas such as laser-based welding and machining, biophotonics, atomic/molecular physics, to list a few. As many laser sources emit a Gaussian beam with a circular cross-section, a common energy inefficient approach of transforming the bell-shaped beam into a flat-top is to either truncate the Gaussian tails or to attenuate the input with a filter having a suitable transmittance profile. Refractive and reflective optical schemes capable of beam shaping are generally more expensive and difficult to fabricate. Moreover, with these elements it is usually difficult to reshape the beam into a range of different profiles. Solutions based on diffractive optical elements such as computer generated holograms [1,2], diffractive gratings [3–5], and binary phase plates [6–9] can be energy efficient. These beam shaping techniques can be broadly classified under two categories, amplitude modulation or phase modulation, where those based on phase modulation are more energy efficient, with conversion efficiencies reaching as high as 95% [10–13]. In addition, the usually static phase objects employed in such techniques have low absorption coefficients and thus are convenient for high power beam shaping applications [6].

An ideal beam shaping technique should be, first and foremost, energy efficient. This implies, particularly in the case of shaping Gaussian beams, redirecting the photons from the tails into targeted regions closer to the optical axis. In addition, it should be easy to reshape the input beam profile into arbitrarily desired lateral profiles with minimum or no computational effort involved. The intensity landscapes should be speckle-free and hence should not be realized as an array of discrete diffractive spots. The emerging wavefronts should be as flat as possible and simple and robust binary-only phase modulation should be applicable. All of the above mentioned ideal requirements can be addressed by using the Generalized Phase Contrast technique (GPC) [14].

GPC which is a pure phase modulation technique can be considered as a full wavelength extension of the pioneering work by Zernike [15] to visualize weak phase objects. GPC provides a relatively simple analytical framework for the optical system under consideration

and is very useful for optimizing experimental parameters. The technique has been explored at length and has demonstrated its utility in diverse fields such as optical trapping and manipulation [16–18], neuro-photonics and optogenetics [19], optical cryptography [20,21] and wavefront sensing [22]. With GPC, there is a direct mapping from the input phase to the output intensity distribution and this facilitates a virtually computation-free design of phase elements. This is particularly pertinent for arbitrary lateral beam shaping. Other beam shaping techniques require exhaustive and time-consuming computations [1,9–10] and are more prone to errors. In the case of static applications, GPC-based beam shaping is less susceptible to fabrication errors. By spatially encoding the input beam with a proper phase, GPC can channel the energy from the tails of a Gaussian into the central beam region with a minimal loss of photons. An added advantage with GPC is that the output light-fields are speckle-free and can have a flat output phase, unlike diffractive techniques, as recently demonstrated experimentally using SLM-based dynamic shaping for neuron stimulation [19].

Figure 1 shows a generic GPC beam shaping setup using two phase plates at the input and Fourier planes. Working as a common-path interferometer, it creates an image of the phase object at the output and simultaneously synthesizes its own reference wave, using an optimized phase contrast filter (PCF), to transform the phase image into a high-contrast intensity pattern that resembles the phase pattern. In this paper we demonstrate, for the first time, the experimental application of GPC to tailor Gaussian beams into a range of different geometric shapes with near flat-top intensity distributions. Section 2 demonstrates the use of GPC for SLM-based Gaussian beam shaping to create arbitrary intensity patterns. In Section 3, we explore the feasibility of a self-contained beam shaper by replacing the SLM with fabricated fixed phase plates designed based on our previous numerical simulations [23]. We elaborate on the fabrication of the binary-phase elements and discuss the role played by critical components. We conclude in section 4 by highlighting possible improvements and other novel applications.

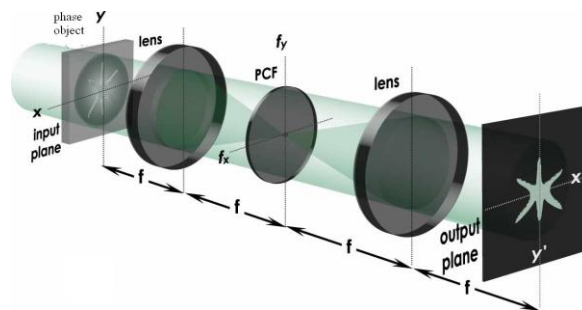


Fig. 1. A typical Gaussian beam-shaping Generalized Phase Contrast (GPC) setup. An optimized phase contrast filter (PCF) simultaneously creates an image of the phase object and a co-propagating reference wave that transform this into a high-contrast interference pattern. Without any intrinsic randomness, this image-and-interfere scheme is inherently speckle-free.

## 2. Reconfigurable beam shaping using a Spatial light modulator

To demonstrate reconfigurable beam shaping, we created different phase objects by displaying computer-generated video patterns (800×600 SVGA resolution) on a phase-only SLM (Hamamatsu Photonics). The phase objects are illuminated by an expanded Gaussian beam from a Ti:Sapphire laser ( $\lambda=830\text{nm}$ , Spectra Physics 3900s, pumped by a Nd:YVO4 Spectra Physics Millennia) and used as input for the GPC beam shaper. The output beam is imaged by a CCD camera and digitized by a frame grabber for beam analysis. For real-time reconfigurable beam shaping, an optimum efficiency should be obtained for different patterns without changing the phase contrast filter (PCF). To test this possibility, we used  $\pi$ -shifting PCFs with different sizes (fabricated on a single glass plate) and analyzed how the PCF size affects the efficiency of the different beam patterns. Figure 2 plots the efficiency of the various patterns for different PCF sizes. The efficiency,  $\eta$ , is calculated as

$\eta = \sum_{m \in \text{target}} I_m / \sum_{n \in \text{Gaussian}} I_n$ , which is the ratio of the total pixel intensity within the target shape to the total pixel intensity for the Gaussian input. The plot shows that, although the peak efficiency varies for different patterns, a consistent efficiency may be obtained using a single PCF size (40 $\mu\text{m}$ ).

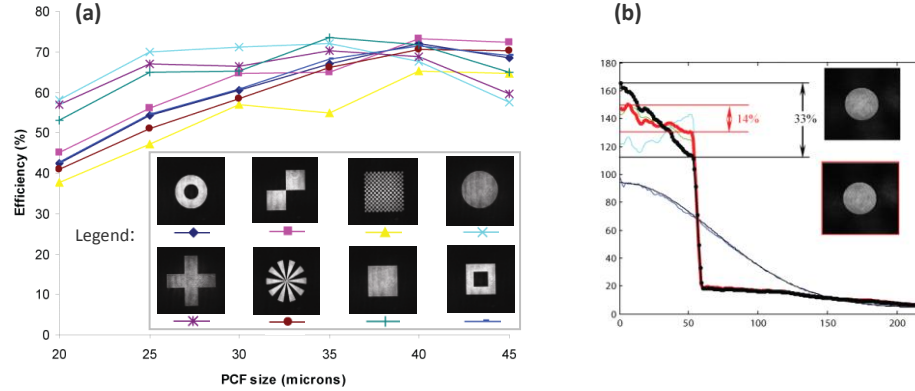


Fig. 2. Efficiency and beam uniformity in GPC-based Gaussian beam shaping: (a) Efficiency of different beam patterns vs. PCF size. The displayed legend shows experimentally obtained beam patterns for a 40 $\mu\text{m}$  PCF size. (b) Radial variation of the intensity for a circular beam shows a 30% intensity rolloff. This rolloff is reduced to 14%, without losing efficiency, using input phase corrections.

Our previous numerical results [23] predict a residual intensity rolloff in GPC-based beamshaping. This rolloff is shown in Fig. 2(b), which plots the radial variation of the intensity for a circular pattern. The intensity plotted at each radial distance is averaged over all pixels located at that distance away from the center of the beam. The Gaussian input is also shown for reference. We have earlier proposed [24] to minimize this roll-off by correcting the input phase to lower the encoded phase in the brighter regions of the pattern. A reconfigurable SLM is well-suited for this correction, which is not suitable for real-time operation. Here we illustrate that some roll-off improvement can be attained through input phase corrections using the same  $\pi$ -PCF. The corrected output and its corresponding radial profile are shown in Fig. 2 (b). The calculated efficiency is maintained during the uniformity correction, which can be understood from Fig. 2(b) since a drop in the central intensity is accompanied by an increase in the peripheral intensity. The background noise is the same in the intensity-flattened and uncorrected patterns.

### 3. Static beam shaping using fixed binary phase plates for high-power applications

#### 3.1 Fabrication of binary phase elements and experimental setup

Although SLMs can generate dynamic phase patterns, they are costly and have low damage thresholds. For static high-power beam shaping, we fabricated low-cost fixed phase elements on a glass substrate to withstand much higher input powers than a typical SLM. We used a cheap technique of printing circular, rectangular and square shapes on a plastic transparency which were photo-lithographically transferred onto a Pyrex substrate spin-coated with 1.5  $\mu\text{m}$  of positive resist. The relief patterns were subsequently developed by chemically etching the wafer in a buffered HF bath (etch rate of  $\sim 80$  nm/min). The dimensions of the phase objects, both at the input and at the Fourier plane, were chosen based on our previous simulations [23]. For example, to reshape the output of a fiber laser into a circular profile, we used a circular  $\pi$ -phase region of radius,  $a_0$ , of  $\sim 0.34w_0$ , where  $w_0$  is  $1/e^2$  radius of the Gaussian beam at the input plane. For generating beams with square or rectangular profiles, their dimensions were estimated by approximating them to the circular object with their aspect ratio made to fit

the input. These patterns were etched to a depth of 1154 nm in a Pyrex wafer (refractive index  $n = 1.464$ ). This depth provides a  $\pi$ -phase shift when illuminated at  $\lambda=1070$  nm. The 5-10% variation in the dimensions of the fabricated phase objects did not substantially lower the conversion efficiency, which shows tolerance to fabrication errors.

The phase contrast filters (PCF) were likewise fabricated. The phase-shifting filter at the Fourier plane is a circular pit of diameter 40  $\mu\text{m}$  and etched to the same depth (1154 nm) as that of the input objects. The PCF design applies the so-called “darkness condition” for plane wave analysis [14], which specifies the matching parameters as:  $\phi_d = 0.4 \times 2.44\lambda f / \phi_{\text{iris}}$ , where  $\phi_d$  is the optimal filter diameter,  $f$  is the focal length of the Fourier lens (L3) and  $\phi_{\text{iris}} = 2a_0$  is the diameter of the iris located at the input plane. Using the correct filter size is crucial for obtaining a high conversion efficiency since even suboptimal filters can yield good contrast, but with much lower conversion efficiencies.

The beamshaping setup is illustrated in Fig. 3. We replaced the Ti:Sapphire laser with a fiber laser (IPG Laser GmbH) for a compact, high-power illumination (typically at 10W). The laser beam is first expanded and collimated by a Galilean telescope (lenses L1 and L2) before illuminating the phase object. The phase contrast filter is located at the Fourier plane between the two lenses L3 and L4. The output intensity distribution at the back focal plane of lens L4 is imaged on the CCD sensor. These images are transferred to a computer for further analysis. Neutral density filters are placed in front of the CCD camera to avoid image saturation. The interference pattern overlaid on the images in Figs. 4 and 5 are artifacts generated by the coating of the optical components in the system.

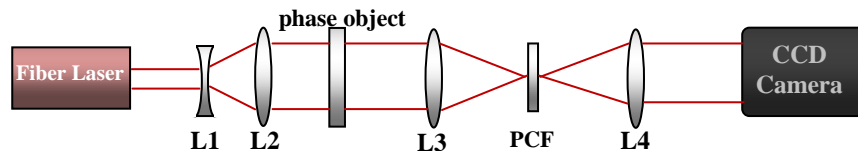


Fig. 3. Schematic diagram of the GPC beam-shaping setup. The input beam is expanded by lenses L1 ( $f_1 = -100\text{mm}$ ) and L2 ( $f_2 = +250\text{mm}$ ). Fourier lenses L3 and L4 both have focal lengths of 200 mm. The PCF is a phase-only filter that creates a  $\pi$ -phase shift over an on-axis circular region (diameter,  $2R \sim 40\mu\text{m}$ ) in the spatial Fourier plane.

### 3.2 Experimental results

Figure 4 shows an example of shaping the Gaussian output from a fiber laser into a circular lateral profile with a near-flat-top intensity distribution.

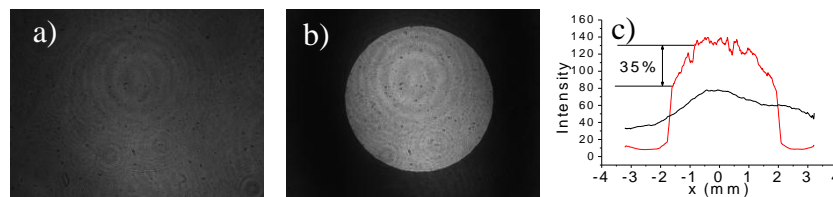


Fig. 4. Shaping of a Gaussian into a near top-hat beam: (a) Output image when the filter in the Fourier plane (FP) is removed; (b) Output image when an optimal filter is inserted to shape the beam into a top-hat; (c) Line scans through Figs. 4a (black) and 4b (red), respectively.

Figure 4a shows the case when the filter in the Fourier plane of the GPC setup is removed. Without the phase filter in place, Fig. 4a shows that the system becomes a standard 4f imaging setup, which only maps the Gaussian from the input and hardly reveals the input phase object. When a phase filter of optimal size is inserted in the Fourier plane, a high contrast image is seen at the output plane, i.e. Figure 4b. The output intensity level in the central region is  $\sim 1.8$  times that of the input beam. The red trace in Fig. 4c refers to a horizontal line scan of the output image which shows a near flat-top intensity distribution within the circular lateral profile. An interesting feature is the steep edges at the output beam in comparison to the input Gaussian shown by the black line profile in Fig. 4c. These sharp

beam transitions can be a desired feature for many applications, especially for laser-based micro-drilling and PCB manufacturing. The line scans through the images elucidate the re-routing of the photons from the tails of the Gaussian into the central region with a desired lateral profile.

Two other examples of static beam-shaping are presented in Fig. 5. In these cases, the Gaussian input beam is reshaped into either square or rectangular beam profiles. Such profiles are useful for efficiently illuminating devices with rectangular cross-sections as for example SLM's [25]. The average experimental efficiency of around 75% is close to the numerical prediction (86%). Thus, GPC-based light-shaping, using binary-phase plates, achieves higher efficiency than binary phase approaches reported in [6–9] and by using a much simpler design that can be easily reconfigured. The maximum intensity variation from the flat top region to the edge of the beam is around 30%. As seen in the previous section, these intensity variations can be minimized by implementing phase corrections [24] onto the input phase objects. Advanced multilevel fabrication techniques would be needed to implement these corrections on fixed phase objects. All in all, in comparison to commercially available beam shaping modules, our results show that GPC is able to arbitrarily shape beams with relatively high conversion efficiencies using very simple binary-phase optics.

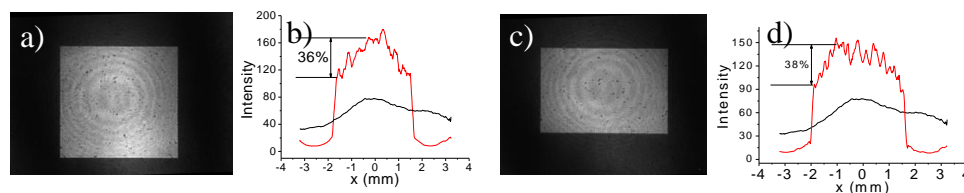


Fig. 5. a) and c) are square and rectangular profiles obtained by shaping the circular Gaussian beam. 5b and 5d are the line scans through the respective images. The red line indicates the horizontal scan through the reshaped profile and the black trace is that of the input Gaussian.

#### 4. Conclusions and outlook

We have experimentally demonstrated the shaping of a Gaussian beam into a variety of geometric shapes. We showed arbitrary beam shaping using dynamic phase patterns on a phase-only SLM. Implementing our proposed multilevel phase encoding scheme [24,26] smoothens out observed weak intensity variations. Furthermore, we showed a beam shaping GPC-module using fabricated phase plates that can withstand input powers as high as 10W, which can be suitable for high power applications. The results show that GPC achieves high conversion efficiencies, similar to other more complicated beam shaping techniques, by employing simple binary-phase optical elements. The measured experimental conversion efficiencies and the maximum intensity variations are in good agreement to earlier numerical predictions. We envision the potential use of GPC-based beam shaping for ultra-fast light pulses and supercontinuum light sources [27]. We envisage that applications such as high precision surface micro-structuring [28] that today employ less efficient and complicated diffractive elements can greatly benefit from this technique.

#### Acknowledgments

We thank the Danish Technical Scientific Research Council (FTP) for financial support; Elena Khomtchenko and Rune K. Christiansen from DTU Danchip for helping fabricate the binary phase optics; and Peter John Rodrigo for assisting with the SLM-based experiments.